



Research article

Generation of Julia and Mandelbrot fractals for a generalized rational type mapping via viscosity approximation type iterative method extended with s -convexity

Arunachalam Murali and Krishnan Muthunagai*

Department of Mathematics, Vellore Institute of Technology, Chennai, 600127, Tamil Nadu, India

* **Correspondence:** Email: muthunagai@vit.ac.in.

Abstract: A dynamic visualization of Julia and Mandelbrot fractals involves creating animated representations of these fractals that change over time or in response to user interaction which allows users to gain deeper insights into the intricate structures and properties of these fractals. This paper explored the dynamic visualization of fractals within Julia and Mandelbrot sets, focusing on a generalized rational type complex polynomial of the form $S_c(z) = az^n + \frac{b}{z^m} + c$, where $a, b, c \in \mathbb{C}$ with $|a| > 1$ and $n, m \in \mathbb{N}$ with $n > 1$. By applying viscosity approximation-type iteration processes extended with s -convexity, we unveiled the intricate dynamics inherent in these fractals. Novel escape criteria was derived to facilitate the generation of Julia and Mandelbrot sets via the proposed iteration process. We also presented graphical illustrations of Mandelbrot and Julia fractals, highlighting the change in the structure of the generated sets with respect to the variations in parameters.

Keywords: escape criterion; Julia set; Mandelbrot set; viscosity approximation type iterative technique

Mathematics Subject Classification: 28A80, 37F10, 39B12

1. Introduction

Fractal geometry challenges the notion of nature conforming to simple shapes, revealing its complexity through irregular patterns. It offers a versatile framework to analyze intricate forms that defy traditional geometric categorization. By embracing self-similarity across scales, fractal geometry provides insights into the ordered yet seemingly chaotic shapes found in nature. Through fractals, we explore the beauty inherent in irregular shapes, challenging conventional ideas of simplicity. This holistic approach allows a deeper understanding of the principles governing natural complexity. Fractal analysis spans diverse fields, from science to art, enriching our perception of the world. It unveils the underlying unity in seemingly disparate patterns, inviting exploration of nature's intricacies. For more

details, refer to [1, 2].

The fascination with fractals, notably the Mandelbrot and Julia sets, has been a long-standing pursuit in mathematics. While the concept of Julia sets originated from the work of French mathematicians Pierre Fatou [3] and Gaston Julia [4] in the early 20th century, it wasn't familiar until in the late 1970s with the advent of computers that their intricate visual representations became possible. Benoit Mandelbrot [5], a key figure in fractal geometry, notably pioneered the visualization of these fractals, particularly by plotting the Julia set for the quadratic form of $z^2 + c$, where c is a complex number. Since then, the exploration of Mandelbrot and Julia sets has expanded, driving further research into the rich world of fractals.

The formation of fractals, particularly the Mandelbrot and Julia sets, owes much to several fixed-point iteration approaches. These approaches, crucial for their development, can generally be categorized into two ways: the Mann-type iteration scheme [6] and the Halpern-type iteration scheme. The Mann process, known as an averaged iterative approach, has undergone modifications over time to ensure strong convergence, reflecting ongoing efforts to refine fractal generation techniques. On the other hand, Halpern [7] introduced a novel iterative method in 1967 specifically for approximating fixed points of non-expansive maps. This innovation laid the foundation for subsequent advancements, notably the viscosity approximation method pioneered by Moudafi [8]. Since its inception, the viscosity method has found widespread application in locating fixed points of non-expansive mappings and other nonlinear functions. Mainge further contributed to this field by exploring the convergence of the viscosity method, particularly concerning the computation of fixed points within the broader class of quasi-non-expansive mappings. Such iterative approaches have significantly advanced the study and application of fractals, enriching our understanding of their intricate structures.

The exploration of fractals, notably the Julia and Mandelbrot sets, has been greatly enriched by the application of diverse iterative techniques across different studies. Romera et al. [9] used the Picard iterative method for exploration of fractals in complex polynomials. In 2020, Abbas et al. [10] brought a deeper understanding about the behavior of complex polynomials. By harnessing the Picard Ishikawa orbit methodology, they discerned escape criteria for a range of complex polynomials, including quadratics, cubics, and polynomials of higher degrees. The authors of [11] present a new perspective on visualizing the Mandelbrot and filled-in Julia sets for the function $z^2 + c$ which involves integrating a constant Möbius transformation at every iteration step. Their investigation specifically delves into the exploration of affine and inverse Möbius transformations.

Authors of [12] investigated the behavior of a broadened transcendental entire function through the application of the Mann iteration process. Qi et al. [13] showcased fixed-point results for sine functions employing different iterations. In [14] complex polynomials with cosine and sine functions have been calculated using the Picard–Mann method. In another instance, authors of [15] utilized a four-step iteration equipped s -convexity to elucidate the Mandelbrot and Julia sets of complex cosine polynomial functions. In [16], Rawat et al. generated and analyzed eye-catching fractals using the Phuengrattana and Suantai (SP) iteration scheme equipped with s -convexity by the polynomial $az^n + \frac{b}{z^m} + c$. For more details on recent studies on exploration of the Mandelbrot and Julia sets, see [17, 18].

In recent publications, Kumari et al. [19] explored the application of viscosity-type approximation methods in fractal generation. Furthermore, in [20], Kumari et al. investigated a generalized viscosity approximation methodology suggested by Nandal et al. in [21], focusing on its utility in generating Mandelbrot and Julia sets. In their study detailed in [22], researchers employed the viscosity

approximation iteration process to analyze and visualize the dynamics of Julia and Mandelbrot sets. They focused on analyzing and visualizing complex polynomials of the form $z^n + bz + c$, where $n \geq 2$ and $b, c \in \mathbb{C}$, shedding light on the intricate behaviors of these fractals. Additionally, they introduced two numerical measures enabling the analysis of how changes in set shape correlate with variations in the iteration parameters.

In the process of fractal generation, researchers have extensively explored various iteration processes derived from fixed point theory. However, there has been limited attention given to methods like Halpern or viscosity type approximation, especially concerning complex fractals. Even if such studies exist, they often focus solely on conventional complex polynomial mappings. Given the burgeoning volume of research work over the last few years focusing on the viscosity approximation techniques within fixed point theory, we are prompted to explore its broader potential beyond traditional applications. Specifically, we believe this method holds significant promise for diverse applications, including the generation of fractals.

Building on this approach and inspired by the wide-ranging applications of complex polynomials, our work extends viscosity approximation iteration processes to include s -convexity for rational-type complex polynomial functions. Unlike traditional studies that concentrate on escape criteria for normal complex functions, our study employs a generalized rational-type complex polynomial approach. By incorporating viscosity approximation with iteration extended by s -convexity, we gain greater control over the morphology of the resulting sets.

In this work, we investigate the dynamic visualization of fractals within the Julia and Mandelbrot sets, particularly focusing on a generalized rational-type complex polynomial described by $S_c(z) = az^n + \frac{b}{z^m} + c$. Here, $a, b, c \in \mathbb{C}$ with $|a| > 1$ and $m \geq 1, n > 1$. By employing a viscosity approximation type orbit extended with s -convexity, we unravel the intricate dynamics inherent in these fractals. We introduce innovative escape criteria to facilitate the generation of Mandelbrot and Julia sets using the proposed iteration process. Graphical illustrations of Mandelbrot and Julia fractals, indicate how the variations in iteration and contraction parameters significantly affect their formation. These examples vividly demonstrate the clear exploration of both sets on the specifics of the iterative process, revealing changes in their complexity, shape, and visual patterns. Through this visual documentation, we aim to deepen our understanding of the intricate relationship between parameter adjustments and the emergent properties of these fascinating fractal structures.

The article comprises of two sections apart from the introduction and conclusion. The second section revisits the prerequisites that are needed for our work. In Section 3, one can find the algorithms used, figures representing the Julia and Mandelbrot sets generated for various parameters, results, and discussions.

2. Preliminaries

In this section, we revisit several fundamental concepts that play a crucial role throughout the entirety of this paper.

Definition 2.1. [4] *The filled Julia set (F_{S_c}) is defined as follows. S_c denotes a polynomial function with complex coefficients, mapping complex numbers to complex numbers, where $c \in \mathbb{C}$ is a parameter*

$$F_{S_c} = \{z \in \mathbb{C} : \{\|S_c^p(z)\|\}_{p=0}^{\infty} \text{ is bounded}\}, \quad (2.1)$$

and where $S_c^p(z)$ represents the p th time composition of S_c .

Definition 2.2. [5] Let $S_c : \mathbb{C} \rightarrow \mathbb{C}$ be a complex-valued polynomial function, with the parameter $c \in \mathbb{C}$. The Mandelbrot set M encompasses all complex numbers $c \in \mathbb{C}$ where the associated filled Julia set F_{S_c} exhibits connectivity, i.e.,

$$M = \{c \in \mathbb{C} : F_{S_c} \text{ is connected}\}. \quad (2.2)$$

According to [16], M can also be defined as

$$M = \{c \in \mathbb{C} : |S_c^p(\theta)| \rightarrow \infty \text{ as } p \rightarrow \infty\}.$$

The starting point θ is chosen such that $S_c'(\theta) = 0$, indicating that θ is a critical point of S_c .

Definition 2.3. [23] Consider a nonempty set A and $z_1, z_2, \dots, z_n \in A$, $s \in (0, 1]$. The s -convex combination of the elements z_1, z_2, \dots, z_n can be represented as:

$$p_1^s z_1 + p_2^s z_2 + \dots + p_n^s z_n, \quad (2.3)$$

where $p_i \geq 0$, for $i \in \{1, 2, \dots, n\}$ and $\sum_{k=1}^n p_k = 1$.

The pioneering investigation into the viscosity approximation method dates back to Moudafi's [8] in 2000. This approach, operating within the complex plane, is delineated in the following.

Definition 2.4. Let $S : \mathbb{C} \rightarrow \mathbb{C}$ denote a complex-valued polynomial mapping. Define a sequence z_i as follows:

$$z_{i+1} = p_i g(z_i) + (1 - p_i) S(z_i), \quad i \geq 0, \quad (2.4)$$

where $z_0 \in \mathbb{C}$ serves as the initial point, $p_i \in (0, 1)$, and g represents a self contraction mapping on \mathbb{C} . This sequence z_i is referred to as the viscosity approximation method.

Mainge [24] proposed a modified version of the viscosity approximation approach, which serves as a specialized variant of the formulation discussed previously (2.4). Initially, the sequence z_i is initiated from an arbitrary point $z_0 \in \mathbb{C}$, and it evolves according to the recurrence relation given by:

$$z_{i+1} = p_i g(z_i) + (1 - p_i) S_q z_i, \quad i \geq 0. \quad (2.5)$$

Here, $S_q = qI + (1 - q)S$, where S represents a quasi-non-expansive mapping and I denotes the identity mapping. The parameters p_i and q are constrained to lie in the interval $(0, 1)$.

In the domain of the complex plane, Sudesh Kumari et al. [22] explored a viscosity approximation-type orbit z_i proposed by Mainge, as follows:

$$\begin{aligned} z_{i+1} &= p_i g(z_i) + (1 - p_i) y_i, \\ y_i &= q z_i + (1 - q) S_c(z_i), \quad i \geq 0, \end{aligned} \quad (2.6)$$

where $z_0 \in \mathbb{C}$ serves as the initial point, S_c represents a complex polynomial function, $g : \mathbb{C} \rightarrow \mathbb{C}$ is a contraction condition, and $p_i, q \in (0, 1)$ are parameters. They considered the complex polynomial

$$S_c(z) = z^n + bz + c, \quad (2.7)$$

where $n \geq 2$ and $b, c \in \mathbb{C}$. Furthermore, they used a complex contraction such that $g(z) = \alpha z + \beta$, with $\alpha, \beta \in \mathbb{C}$ satisfying $|\alpha| < 1$.

Definition 2.5. The viscosity filled Julia set F'_{S_c} of S_c , as defined in Eq (2.7), is characterized by the set

$$F'_{S_c} = \{z_0 \in \mathbb{C} : \{z_i\}_{i=0}^{\infty} \text{ is bounded} \},$$

where z_i follows the definition provided in Eq (2.6). The viscosity Julia set J'_{S_c} of S_c comprises of the boundary points of the viscosity filled Julia set F_{S_c} , denoted as $J'_{S_c} = \partial F'_{S_c}$.

Definition 2.6. Consider the function S_c defined by Eq (2.7), where $c \in \mathbb{C}$ serves as a parameter. Defining the viscosity Mandelbrot set M_c as

$$M_c = \{c \in \mathbb{C} : |z_i| \rightarrow \infty \text{ as } i \rightarrow \infty\},$$

with $z_0 = 0$ and z_i , for $i > 0$ governed by Eq (2.6) of S_c .

The iterations involving z are written inside M_c because the boundedness of the sequence $\{z_i\}$ under the function S_c is used to determine whether the parameter c belongs to the Mandelbrot set M_c . The behavior of z iterations reflects the influence of c , making it an essential part of the set's definition. For simplicity, we adopt the convention $p_i = p$, with $p \in (0, 1)$, throughout the article.

3. Viscosity approximation type iteration extended with s-convexity for a generalized rational type complex polynomial mapping

In literature, we encounter various extensions of the convex combination concept. One notable example is the s-convex combination. Here, we blend the classic convex combination concept with the s-convex method in viscosity approximation type orbit. In this article, we examine the subsequent orbit of viscosity approximation type equipped with s-convexity for a generalized rational type complex polynomial mapping S and a complex contraction condition g :

$$\begin{aligned} z_{i+1} &= p^s g(z_i) + (1-p)^s y_i, \\ y_i &= q^s z_i + (1-q)^s S_c(z_i), \end{aligned} \quad (3.1)$$

where $z_0 \in \mathbb{C}$ serves as the initial point, S_c represents a complex polynomial, $g : \mathbb{C} \rightarrow \mathbb{C}$ is a contraction mapping, and $s \in (0, 1]$, $p, q \in (0, 1)$. Here, we consider the generalized rational type complex polynomial,

$$S_c(z) = az^n + \frac{b}{z^m} + c, \quad (3.2)$$

where $a, b, c \in \mathbb{C}$ with $|a| > 1$, $m, n \in \mathbb{N}$ with $n > 1$ and complex contraction $g(z) = \alpha z + \beta$, where $\alpha, \beta \in \mathbb{C}$ with $|\alpha| < 1$.

The generalized rational map is classified within a more intricate category of complex functions, primarily because the point $z = \infty$ does not serve as an attracting fixed point for this map. By setting $a = 1$, $c = 0$, and $m = n$ in (3.2), the map simplifies to a rational form in [25] given by $f_b(z) = z^n + \frac{b}{z^n}$, where $b \in \mathbb{C}$ and $n \geq 2$.

Remark 3.1. The viscosity approximation type orbit equipped with s-convexity becomes

- 1) The viscosity approximation-type orbit of [22] for $s = 1$.
- 2) The viscosity approximation-type orbit of [24] for $s = 1$ and $q = 0$.

Definition 3.1. The viscosity filled Julia set F'_{S_c} of S_c , defined in Eq (3.2), is characterized by the set

$$F'_{S_c} = \{z_0 \in \mathbb{C} : \{z_i\}_{i=0}^{\infty} \text{ is bounded} \},$$

where z_i follows Eq (3.1). The viscosity Julia set J'_{S_c} of S_c consists of the boundary points of the viscosity filled Julia set F'_{S_c} , denoted by $J'_{S_c} = \partial F'_{S_c}$.

Definition 3.2. Consider the function S_c defined by Eq (3.2), where $c \in \mathbb{C}$ serves as a parameter. The viscosity Mandelbrot set M_c is defined as

$$M_c = \{c \in \mathbb{C} : |z_i| \rightarrow \infty \text{ as } i \rightarrow \infty\},$$

with z_i for $i > 0$ governed by Eq (3.1) of S_c .

Even when the function is not well-defined at $z = 0$, the parameter c is still selected based on the behavior of the iterations starting from a critical point. The extension of the s -convex combination viscosity approximation type iteration to Julia and Mandelbrot sets represents a significant advancement in the study of complex dynamical systems. Julia and Mandelbrot sets are fundamental objects in the field of complex dynamics, providing deep insights into the behavior of iterated functions in the complex plane. One of the primary benefits of this extension is the enhanced ability behaviors during graphical exploration of the complex polynomial within Julia and Mandelbrot sets.

3.1. Escape criterion

In fractal analysis, researchers have explored diverse techniques like escape time algorithms, potential functions, distance estimator algorithms for constructing and analyzing fractals, and iterated function systems [26]. Among these methods, the escape time criteria stands out as one of the most pivotal approaches in fractal generation. At its core, the escape criterion serves as a fundamental condition enabling us to discern whether the trajectory of an initial point veers toward infinity or remains bounded.

The escape criterion plays a major role in analyzing Julia and Mandelbrot sets because it determines how iterations of complex functions are handled. In both sets, points are iterated using certain mathematical functions, and the escape criterion determines when to stop iterating. The escape criterion serves as a termination condition for iterating complex functions, allowing us to classify points in the complex plane as either belonging to or escaping from the Julia and Mandelbrot sets. It is essential for generating accurate visual representations and studying the intricate fractal structures of these sets.

Now, we formulate a comprehensive escape criterion suitable for constructing the viscosity of Julia and Mandelbrot sets. This criterion is designed to accommodate viscosity approximation-type orbits extended with s -convexity, incorporating complex contractions and generalized rational-type complex polynomial mappings.

Theorem 3.1. Let $S_c(z) = az^n + \frac{b}{z^m} + c$ be a generalized rational type complex polynomial of degree n and $g(z) = \alpha z + \beta$ a complex contraction, where $\alpha, \beta \in \mathbb{C}$ with $|\alpha| < 1$. Assume that

$$|z_0| \geq \max\{|c|, |\beta|\} > \left(\frac{2 + sp}{(1 - sp)(1 - sq)(|a| - 1)} \right)^{\frac{1}{n-1}}, \quad (3.3)$$

and $|z_0| \geq |b|^{\frac{1}{n+m}}$, where $a, b, c \in \mathbb{C}$ with $|a| > 1$, $m, n \in \mathbb{N}$ with $n > 1$. Define a sequence $\{z_n\}$ as follows:

$$\begin{aligned} z_{i+1} &= p^s g(z_i) + (1-p)^s y_i, \\ y_i &= q^s z_i + (1-q)^s S_c(z_i), \end{aligned} \quad (3.4)$$

for $i \geq 0$, $s \in (0, 1]$ and $p, q \in (0, 1)$. Then, $|z_i| \rightarrow \infty$ as $i \rightarrow \infty$.

Proof. Consider the sequence defined by (3.4),

$$\begin{aligned} |y_0| &= |q^s z_0 + (1-q)^s S_c(z_0)| \\ &= |q^s z_0 + (1-q)^s (az_0^n + \frac{b}{z_0^m} + c)|. \end{aligned}$$

By utilizing the binomial expansion of $(1-q)^s$ up to the linear terms of q and considering the inequality $q^s \geq sq$, we obtain

$$\begin{aligned} |y_0| &\geq |sqz_0 + (1-sq)(az_0^n + \frac{b}{z_0^m} + c)| \\ &\geq |(1-sq)(az_0^n + \frac{b}{z_0^m} + c)| - sq|z_0| \\ &\geq (1-sq)|(az_0^n + c)| - (1-sq)|\frac{b}{z_0^m}| - sq|z_0|. \end{aligned}$$

By our assumption $|z_0| \geq \max\{|c|, |\beta|\}$, it follows that $|z_0| \geq |c|$. Furthermore, from the assumption $|z_0| \geq |b|^{\frac{1}{n+m}}$, we get

$$\begin{aligned} |y_0| &\geq (1-sq)|az_0^n| - (1-sq)\left|\frac{z_0^{n+m}}{z_0^m}\right| - (1-sq)|z_0| - sq|z_0| \\ &= (1-sq)|az_0^n| - (1-sq)|z_0^n| - |z_0|. \\ \implies & \\ |y_0| &\geq |z_0|[(1-sq)(|a|-1)|z_0^{n-1}| - 1]. \end{aligned} \quad (3.5)$$

Using Eq (3.4), the binomial expansion of $(1-p)^s$ up to the first-order terms of p , and the inequality $p^s \geq sp$, we arrive at

$$|z_1| \geq |sp(\alpha z_0 + \beta) + (1-sp)y_0|.$$

This leads us to

$$\begin{aligned} |z_1| &\geq (1-sp)|y_0| - sp|\alpha z_0| - sp|z_0| \\ &> (1-sp)|y_0| - sp|z_0| - sp|z_0|, \end{aligned}$$

as $|z_0| \geq \max\{|c|, |\beta|\}$. Using (3.5), we obtain

$$|z_1| > |z_0|[(1-sp)(1-sq)(|a|-1)|z_0^{n-1}| - sp - 1]. \quad (3.6)$$

Because $|z_0| > \left(\frac{2+sp}{(1-sp)(1-sq)(|a|-1)}\right)^{\frac{1}{n-1}}$, we have

$$(1 - sp)(1 - sq)(|a| - 1)|z_0^{n-1}| - sp - 1 > 1.$$

Thus, there exists a positive real number μ such that

$$(1 - sp)(1 - sq)(|a| - 1)|z_0^{n-1}| - sp - 1 > \mu + 1. \quad (3.7)$$

Using (3.7) in (3.6), we have $|z_1| > (\mu + 1)|z_0|$. With $|z_1|$ being greater than $|z_0|$, we can extend our reasoning by repeatedly applying the same logic such that $|z_i| > (\mu + 1)^i|z_0|$. Hence, $|z_i| \rightarrow \infty$ as $i \rightarrow \infty$. \square

We refine the above theorem with the following corollaries.

Corollary 3.1. *Let*

$$|z_0| \geq \max \left\{ |c|, |\beta|, |b|^{\frac{1}{n+m}}, \left(\frac{2 + sp}{(1 - sp)(1 - sq)(|a| - 1)} \right)^{\frac{1}{n-1}} \right\} = R,$$

where $s \in (0, 1]$ and $0 < p, q < 1$. Then, there exists $\mu > 0$ such that $|z_i| > (1 + \mu)^i|z_0|$, and we have $|z_i| \rightarrow \infty$ as $i \rightarrow \infty$.

Corollary 3.2. *Suppose that*

$$|z_j| \geq \max \left\{ |c|, |\beta|, |b|^{\frac{1}{n+m}}, \left(\frac{2 + sp}{(1 - sp)(1 - sq)(|a| - 1)} \right)^{\frac{1}{n-1}} \right\} = R,$$

for some $j \geq 0$, where $s \in (0, 1]$, $0 < p, q < 1$, $a, b, c \in \mathbb{C}$ with $|a| > 1$, and $m, n \in \mathbb{N}$ with $n > 1$. Then, there exists $\mu > 0$ such that $|z_{i+j}| > (1 + \mu)^i|z_j|$, and we have $|z_i| \rightarrow \infty$ as $i \rightarrow \infty$.

Our theorem and corollary underscore the importance of applying s -convexity within viscosity approximation types for generalized rational-type complex polynomials in generating complex fractal sets. Building upon this principal discovery and if the value of s makes a great impact on the shape, we enhance analogous conclusions for viscosity approximation iterations found in existing literature.

3.2. Algorithms

Corollaries 3.1 and 3.2 provide a practical framework for generating both the Julia and Mandelbrot sets associated with the n th degree generalized rational type complex polynomial $S_c(z) = az^n + \frac{b}{z^m} + c$, where $a, b, c \in \mathbb{C}$ with $|a| > 1$, $m, n \in \mathbb{N}$ with $n > 1$. These corollaries offer clear guidelines for determining whether a given point z_0 lies within the filled Julia set or not. If, at any iteration i , the magnitude of z_i surpasses a certain threshold defined by the circle of radius R given by

$$R = \max \left\{ |c|, |\beta|, |b|^{\frac{1}{n+m}}, \left(\frac{2 + sp}{(1 - sp)(1 - sq)(|a| - 1)} \right)^{\frac{1}{n-1}} \right\},$$

then the orbit of $|z_0|$ diverges toward infinity, indicating z_0 is exterior to the filled Julia set. Conversely, if $|z_i|$ remains within this threshold, z_0 is considered to belong to the filled Julia set.

Algorithm 1 delineates the procedural steps for executing the escape time algorithm to generate the Julia set. This approach uses the viscosity approximation orbit extended s -convexity, and incorporates the escape criteria obtained from the above section. The Julia set is constructed within a specified domain $A \subset \mathbb{C}$. To prevent infinite looping, we set a maximum iteration limit of K_1 in the algorithm.

Similarly, Algorithm 2 outlines the process for computing the Mandelbrot set using the viscosity approximation type method orbit extended s -convexity. Like Algorithm 1, it employs the escape criterion outlined in the previous section. The Mandelbrot set is computed within a defined region $A \subset \mathbb{C}$, with a maximum iteration cap of K_1 iterations using the viscosity approximation technique.

In their paper, Kumari et al. [22] presented a detailed pseudo-code outlining the implementation of the escape-time algorithm for generating both the viscosity Mandelbrot and Julia sets. This algorithm operates based on the orbit specified in Eq (2.6) for the complex polynomial $z^n + bz + c$. Here, we give the following algorithms to generate the viscosity Mandelbrot and Julia sets using the orbit defined in (3.1) for the generalized rational type complex polynomial.

Though both Julia sets and Mandelbrot sets are generated through iterative processes involving complex numbers, the main difference lies in the method in which they are constructed (fixed c for Julia sets vs. varying c for Mandelbrot sets) and visualized (for a specific constant c in Julia set, the Mandelbrot set represents the behavior of the iteration).

To create the visual representations of the Julia and Mandelbrot sets showcased in this part, we implement Algorithms 1 and 2 using the MATLAB tool. We also use viscosity approximation orbits extended with s -convexity.

Algorithm 1 Julia set generation

Require: $S_c(z) = az^n + \frac{b}{z^m} + c$, where $a, b, c \in \mathbb{C}$ with $|a| > 1$, $m, n \in \mathbb{N}$ with $n > 1$; $A \subset \mathbb{C}$ –the region from which the set is drawn; The max no. of iterations is denoted by K_1 ; $p, q \in (0, 1)$, the parameters for the viscosity approximation type iterative extended with s -convexity; $s \in (0, 1]$ convexity parameter; $g(z) = \alpha z + \beta$, where $\alpha, \beta \in \mathbb{C}$ & $|\alpha| < 1$; colourmap $[0..K_1]$ – with $K_1 + 1$ colours.

Ensure: Julia set for A .

```

1:  $R = \max \left\{ |c|, |\beta|, |b|^{\frac{1}{n+m}}, \left( \frac{2 + sp}{(1 - sp)(1 - sq)(|a| - 1)} \right)^{\frac{1}{n-1}} \right\}$ 
2: for  $z_0 \in A$  do
3:    $i = 0$ 
4:   while  $|z_i| < R$  and  $i < K_1$  do
5:      $y_i = q^s z_i + (1 - q)^s S_c(z_i)$ 
6:      $z_{i+1} = p^s g(z_i) + (1 - p)^s y_i$ 
7:      $i = i + 1$ 
8:   end while
9:   colour  $z_0$  with colourmap[ $i$ ]
10: end for
```

Algorithm 2 Mandelbrot set generation

Require: $S_c(z) = az^n + \frac{b}{z^m} + c$, where $a, b, c \in \mathbb{C}$ with $|a| > 1$, $m, n \in \mathbb{N}$ with $n > 1$; $A \subset \mathbb{C}$ – area; K_1 – the max no. of iterations; $p, q \in (0, 1)$ – parameters for the viscosity approximation type extended with s -convexity; $s \in (0, 1]$ -convexity parameter; $g(z) = \alpha z + \beta$, where $\alpha, \beta \in \mathbb{C}$ and $|\alpha| < 1$; colourmap $[0 \dots K_1]$ – with $K_1 + 1$ colours.

Ensure: Mandelbrot set for area A .

```

1: for  $c \in A$  do
2:    $R = \max \left\{ |c|, |\beta|, |b|^{\frac{1}{n+m}}, \left( \frac{2 + sp}{(1 - sp)(1 - sq)(|a| - 1)} \right)^{\frac{1}{n-1}} \right\}$ 
3:    $i = 0$ 
4:    $z_0 = c$ 
5:   while  $|z_i| < R$  and  $i < K_1$  do
6:      $y_i = q^s z_i + (1 - q)^s S_c(z_i)$ 
7:      $z_{i+1} = p^s g(z_i) + (1 - p)^s y_i$ 
8:      $i = i + 1$ 
9:   end while
10:  colour  $c$  with colourmap[ $i$ ]
11: end for

```

In Figures 1 and 2, we use hot color maps, utilize an image resolution of 800×800 pixels, and execute a total of 50 iterations for the Julia set and 10 iterations for the Mandelbrot set. To capture finer details and intricate structures in Julia sets, a higher number of iterations, such as $K = 50$, is chosen. This allows for a more accurate representation of the fractal's features. Since determining Mandelbrot set membership involves a binary classification (inside or outside), a lower number of iterations, such as $K = 10$, is often sufficient for a quick assessment of membership. Usage of less numbers of iterations provides a good balance between computational efficiency and capturing the main features of the set.

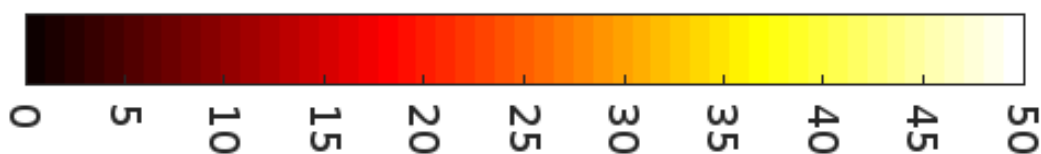


Figure 1. Color maps used to generate the viscosity Julia set example.

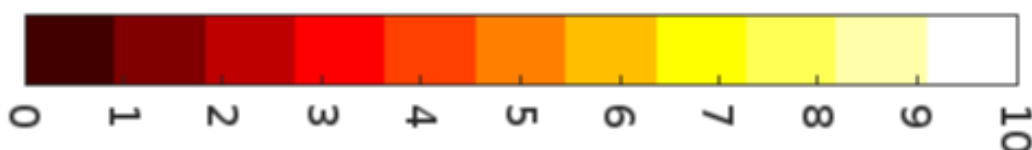


Figure 2. Color maps used to generate the viscosity Mandelbrot set example.

3.3. Examples for the Mandelbrot set

Figure 3 depicts the nature of Mandelbrot set under a generalized rational type mapping. While maintaining the values for parameters $n = 3$, $m = 9$, $a = 3$, $b = -0.0003i$, $\alpha = 0.067$, $\beta = 0.007 - 0.0004i$, $q = 0.92$, and $s = 1$, we systematically vary the value of p across six different settings: (a) 0.11, (b) 0.25, (c) 0.5, (d) 0.62, (e) 0.8, and (f) 0.89.

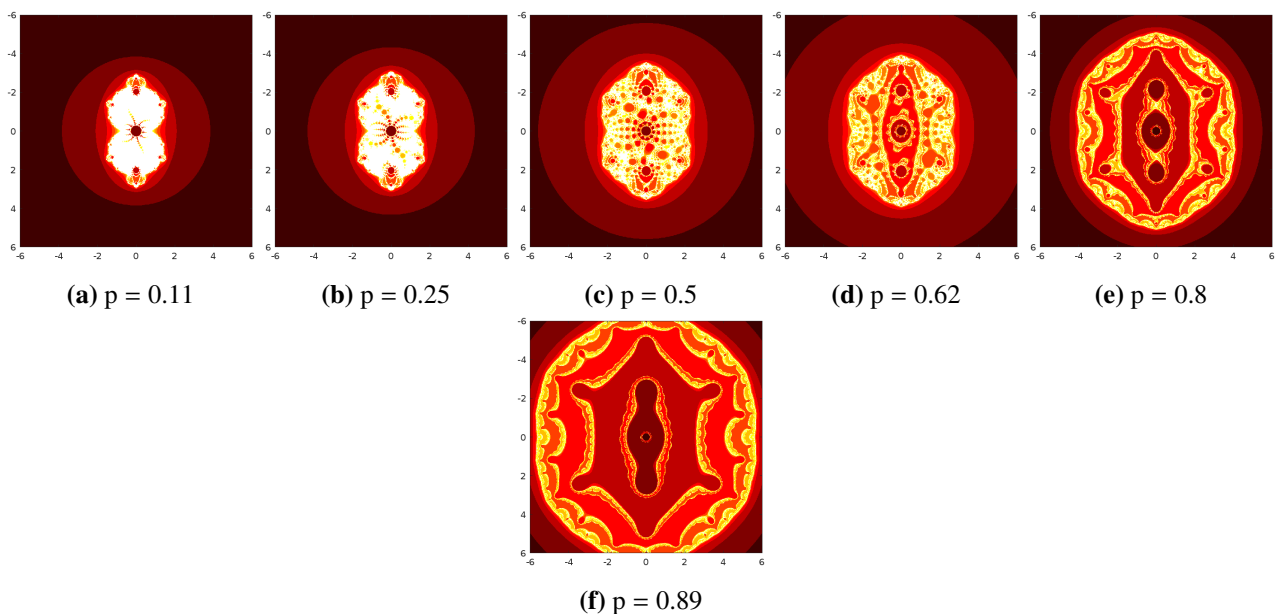


Figure 3. Mandelbrot set for $n = 3, m = 9$ generated using the viscosity approximation type iteration extended with s -convexity by fixing $q = 0.92, s = 1$ and varying p .

Figure 4 represents the Mandelbrot set using a generalized rational mapping technique. Figure 4 is obtained by maintaining the parameters $n = 3$, $m = 2$, $a = 4$, $b = -0.5$, $\alpha = 0.8$, $\beta = -0.4i$, $p = 0.6$, and $s = 0.98$, and varying the value of q across six different settings: (a) 0.22, (b) 0.39, (c) 0.5, (d) 0.7, (e) 0.82, and (f) 0.91.

In Figure 5, we explore the Mandelbrot set using a generalized rational mapping approach. To obtain Figure 5, we keep the parameters $n = 4$, $m = 2$, $a = 2.008$, $b = 1.0008 + .0007i$, $\alpha = 0.85$, $\beta = 0.003 + 0.002i$, $p = 0.69$, and $q = 0.8$ fixed and the value of s is varied across six different settings: (a) 0.1, (b) 0.22, (c) 0.35, (d) 0.5, (e) 0.81, and (f) 1.

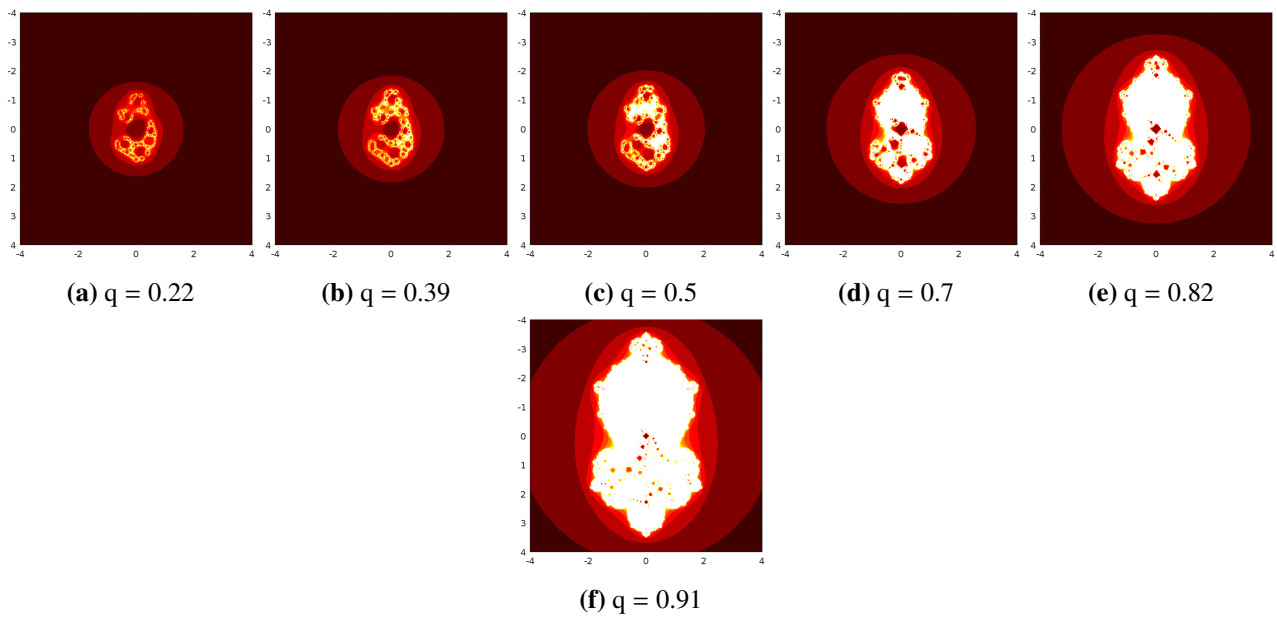


Figure 4. Mandelbrot set for $n = 3, m = 2$ generated through the utilization of the viscosity approximation type iteration extended with s -convexity by fixing $p = 0.6, s = 0.98$ and varying q .

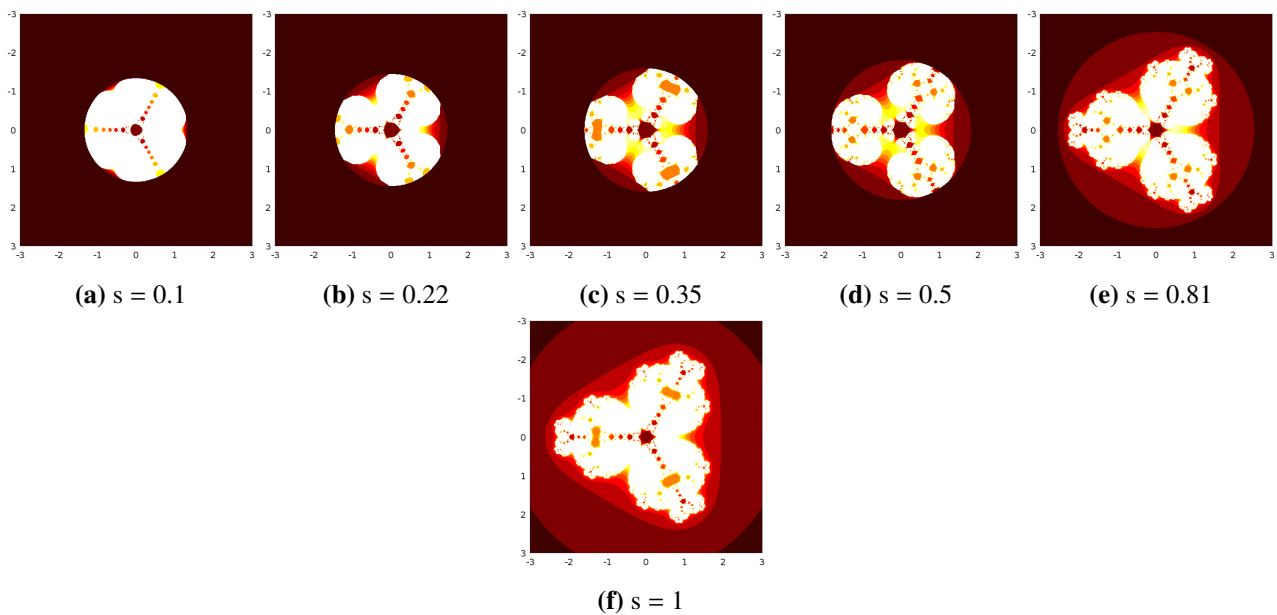


Figure 5. Mandelbrot set for $n = 4, m = 2$ generated by the viscosity approximation method extended with s -convexity. We keep $q = 0.8$ and $p = 0.69$ and vary s .

Subsequently, we move forward to generate a cubic viscosity Mandelbrot set for a generalized rational-type mapping using Algorithm 2. The parameters for generating this set are as follows: $n = 3, m = 9, a = 3, b = -0.0003i, \alpha = 0.067, \beta = 0.007 - 0.0004i$. The illustration showcases a division into three distinct groups.

In the first set, presented in Figure 6, constant values for $q = 0.6$ and $s = 0.7$ are maintained, while the parameter p is varied. Specifically: (a) 0.4, (b) 0.7, and (c) 0.89.

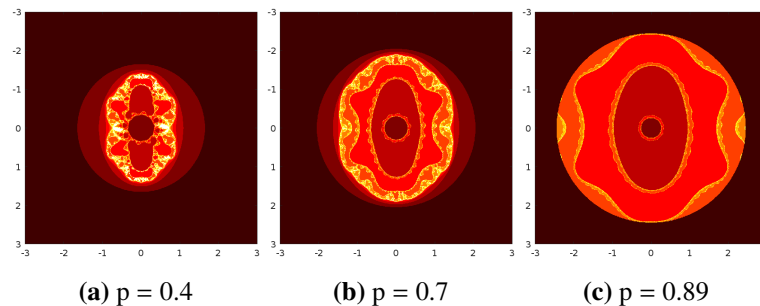


Figure 6. Generating the Mandelbrot set for $n = 3, m = 9$ through the use of a viscosity approximation iteration method, enhanced by incorporating s -convexity, with q set to 0.6 and s to 0.7, while altering p .

In the second set, presented by Figure 7, $p = 0.4, s = 0.89$ are maintained, while the parameter q is varied. Specifically: (a) 0.3, (b) 0.8, and (c) 0.9.

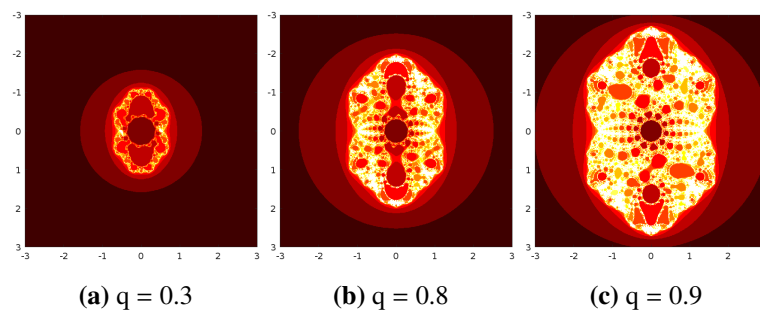


Figure 7. Mandelbrot for $n = 3, m = 9$ generated in way of the viscosity approximation type iteration extended with s -convexity by fixing $p = 0.4, s = 0.89$ and varying q .

In the third set, represented by Figure 8, $p = 0.85, q = 0.3$, and the parameter s is varied. Specifically: (a) 0.4, (b) 0.6, and (c) 1.

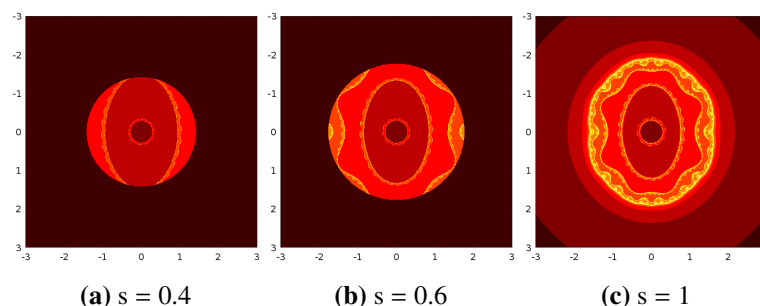


Figure 8. Mandelbrot set for $n = 3, m = 9$ generated using the viscosity approximation type iteration extended with s -convexity, with fixed parameters $p = 0.85$ and $q = 0.3$, while varying s .

Furthermore, we need to show the impact of α, β on the Mandelbrot set generated. Our parameters

$n = 3, m = 2, a = 4, b = 0.7, s = 1, q = 0.6, p = 0.9$, and $\alpha = 0.6$ remain fixed and we adjust the value of β across three settings: (a) 0.99, (b) $1.899i$, (c) $2.899i$. Figure 9 is the visualization obtained by fixing $\alpha = 0.6, s = 1$ and varying the value of β .

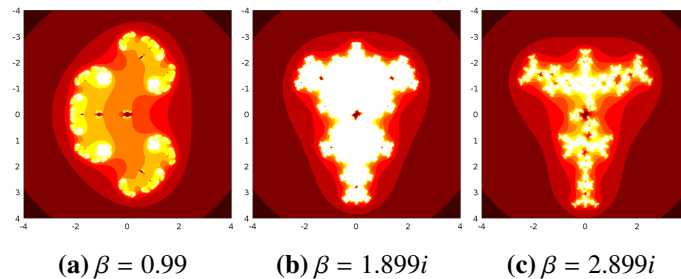


Figure 9. Mandelbrot for $n = 3, m = 2$ generated through the use of the viscosity approximation type iteration extended with s -convexity by fixing $\alpha = 0.6, s = 1$ and varying β .

Next, the parameters $n = 3, m = 2, a = 4, b = 0.7, s = 1, q = 0.6, p = 0.9$, and $\beta = 0.4$ remain fixed, while we vary the value of α across three settings: (a) 0.033, (b) 0.55, (c) 0.8, and obtain Figure 10.

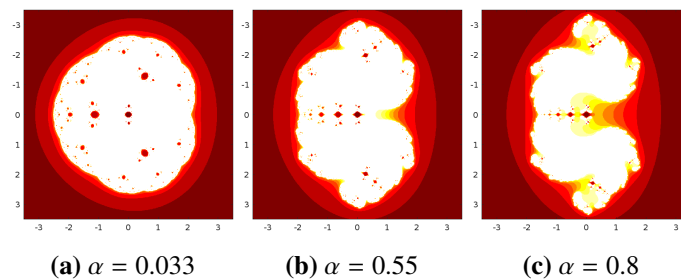


Figure 10. Mandelbrot for $n = 3, m = 2$ generated using an iteration method based on viscosity approximation, augmented with s -convexity, by setting β at 0.4, s at 1, and adjusting α .

We move on to the investigation of the Mandelbrot set for fixed p, q , and s on different values of a, b . Here, we fix the following values $n = 11, m = 9, s = 0.79, q = 0.7, p = 0.9, \alpha = 0.6, \beta = 0.003 + 0.009i$. In Figure 11, to study (a), we use $a = 6, b = 3.098i$. To investigate (b) and (c), we fix $b = 0.004 - 0.005i$ for $a = 2$ and 4.

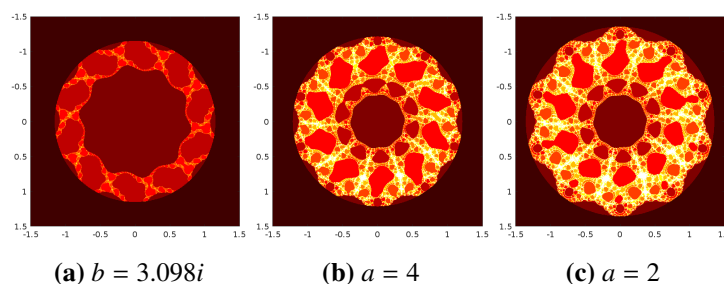


Figure 11. Mandelbrot for $n = 11, m = 9$ generated through the viscosity approximation type iteration extended with s -convexity for different values of a, b .

The generation of the Mandelbrot set using our method is illustrated in Figure 12. Following are the values of the parameter used for Figure 12:

- (a) $n = 6, m = 4, a = 4, b = 0.007 - 0.006i, \alpha = 0.007, \beta = 0.002 - 0.009i, p = 0.79, q = 0.4$, and $s = 0.2$.
- (b) $n = 6, m = 4, a = 4, b = 0.007 - 0.006i, \alpha = 0.007, \beta = 0.002 - 0.009i, p = 0.79, q = 0.4$, and $s = 0.79$.
- (c) $n = 8, m = 4, a = 6, b = 0.809 - 0.906i, \alpha = 0.008, \beta = 2.009 + 1.007i, p = 0.8, q = 0.69$, and $s = 0.7$.
- (d) $n = 11, m = 4, a = 2, b = 0.004 - 0.005i, \alpha = 0.6, \beta = 0.003 + 0.009i, p = 0.2, q = 0.27$, and $s = 0.79$.
- (e) $n = 7, m = 3, a = 2, b = 5, \alpha = 0.08, \beta = 0.0007 - 0.0009i, p = 0.8, q = 0.7$, and $s = 1$.
- (f) $n = 5, m = 3, a = 2, b = 5, \alpha = 0.08, \beta = 0.0007 - 0.0009i, p = 0.8, q = 0.7$, and $s = 1$.

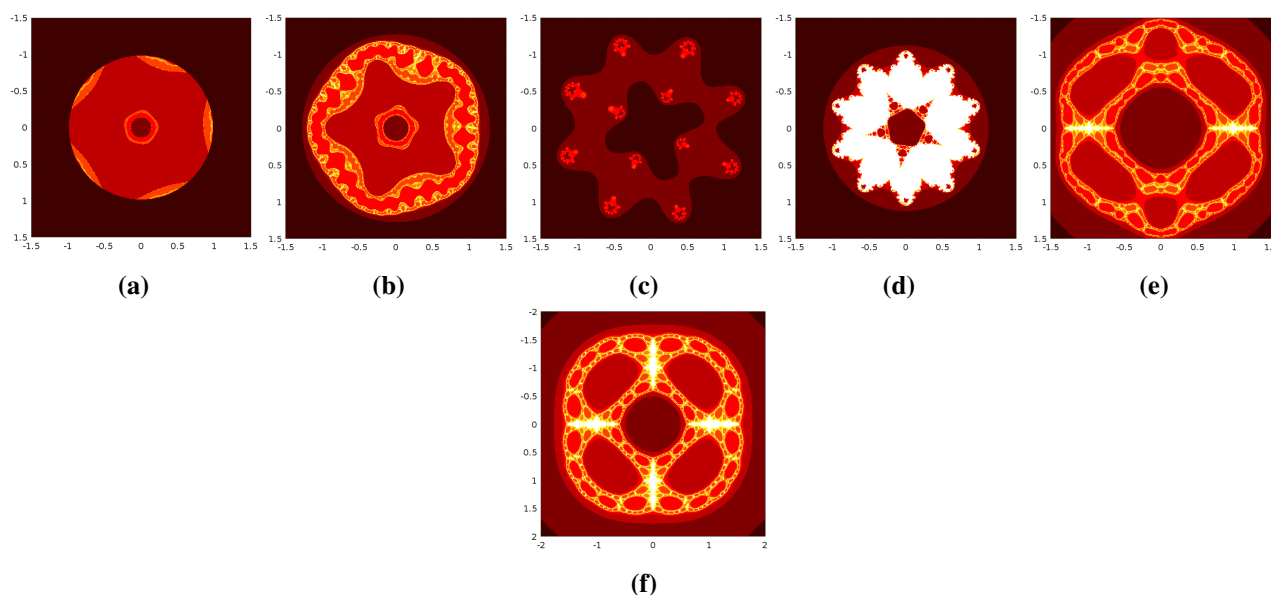


Figure 12. More examples of Mandelbrot sets for viscosity approximation type iteration extended with s -convexity.

3.3.1. Results and discussion on Mandelbrot set

Observing Figures 3 and 4, it becomes evident that both parameters, p and q , significantly influence the shape of the set. As either parameter increases, the set expands and undergoes alterations in its form. Additionally, a noteworthy observation is the axial symmetry present in the resulting sets. Moreover, Figures 6 and 7 highlight a pronounced reliance on the iteration parameters, indicating a substantial impact on the resultant set's configuration. When parameters are set at lower values, the resulting sets appear relatively compact, expanding gradually with parameter increments. From Figures 5 and 8, we can say it's worth noting that a subtle uptick in the value of s brings about a clearer, more comprehensive view, while also infusing additional vibrancy into the fractals. From Figures 9–11, we can see impact of parameters of the contraction and generalized rational type complex polynomial, we can see that the variation in shape is huge, and we obtain sets with different shapes and details.

Observing Figures 3–12, it becomes evident that altering the parameters (especially p, q, s , and α, β) has a profound impact on the shape of the resulting set. As the parameters increase, the set expands in size while simultaneously adopting a more different exploration, thereby sacrificing some of its finer intricacies.

3.4. Examples for the Julia set

In the following part, we examine the Julia set for a generalized rational type condition by utilizing orbits extended with s -convexity under the viscosity approximation method for various input parameters.

In Figure 13, we explore the Julia set for a generalized rational type mapping. The parameters $n = 3, m = 2, a = 4, b = 0.0007 + 0.006i, c = 0.0004 + 0.003i, \alpha = 0.6, \beta = 0.004, q = 0.6$, and $s = 0.4$ remain fixed, while we vary the value of p across six settings: (a) 0.11, (b) 0.25, (c) 0.5, (d) 0.62, (e) 0.7, and (f) 0.85.

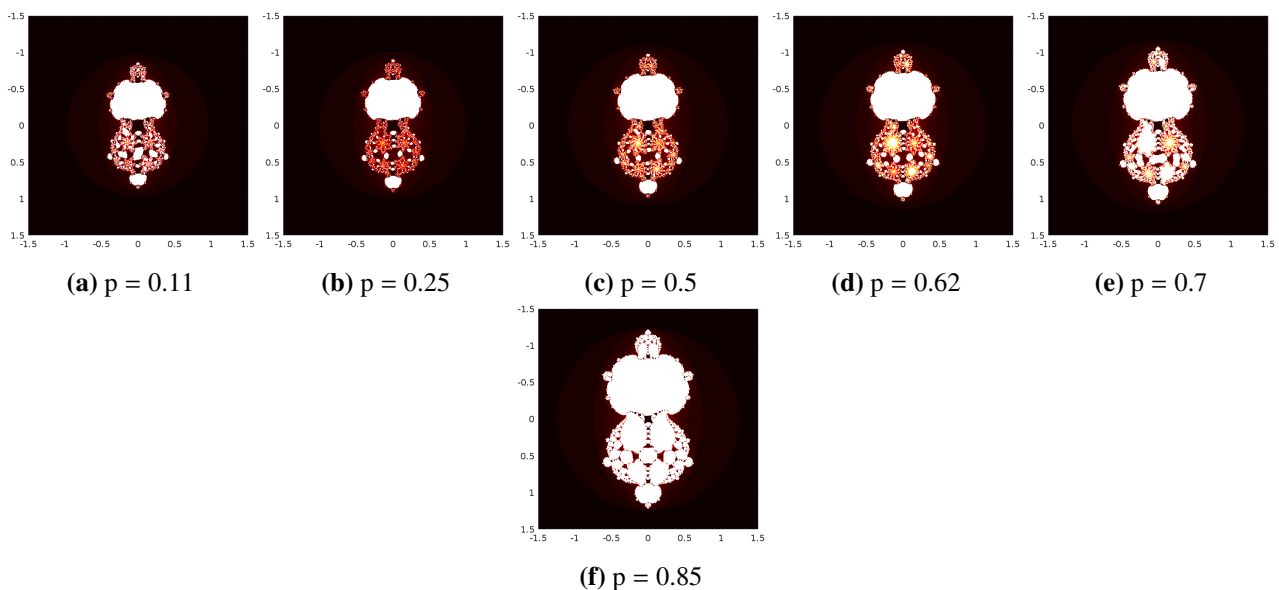


Figure 13. Julia set for $n = 3, m = 2$ generated using viscosity approximation iteration extended with s -convexity, with fixed parameters $q = 0.6$ and $s = 0.4$, while varying p .

Figure 14 illustrates our investigation about the Julia set of a generalized rational-type mapping. While our parameters remain constant ($n = 2, m = 4, a = 3.0004, b = 0.9807 + 0.0009i, c = 0.0006i, \alpha = 0.7, \beta = 0.078 + 0.0056i, p = 0.67$, and $s = 1$), we vary the value of q across six different settings: (a) 0.5, (b) 0.66, (c) 0.73, (d) 0.8, (e) 0.88, and (f) 0.9.

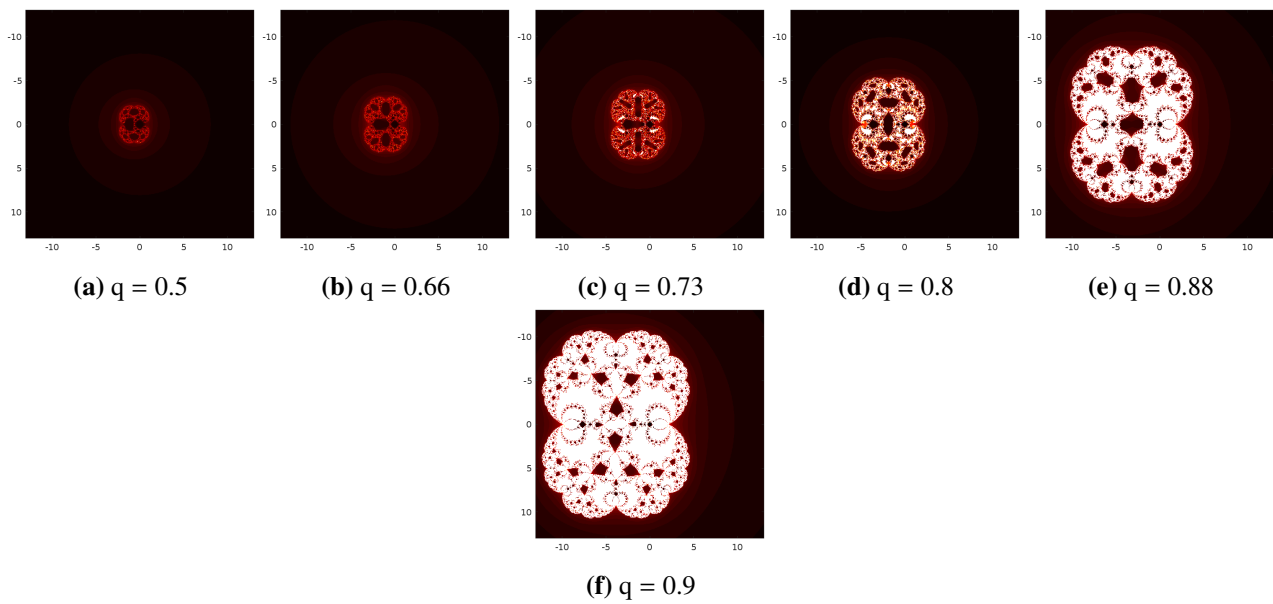


Figure 14. Julia set for $n = 2, m = 4$ generated through the viscosity approximation type orbit extended with s -convexity by fixing $p = 0.67, s = 1$ and varying q .

In Figure 15, we embark on an exploration of the Julia set for a generalized rational-type mapping. We maintain the parameters at fixed values: $n = 2, m = 4, a = 6, b = 1.2i, c = 0.0002i, \alpha = 0.05, \beta = 0.1, p = 0.9$, and $q = 0.9$. However, we introduce variations in the parameter s across six distinct settings: (a) 0.40, (b) 0.56, (c) 0.7, (d) 0.82, (e) 0.95, and (f) 1.

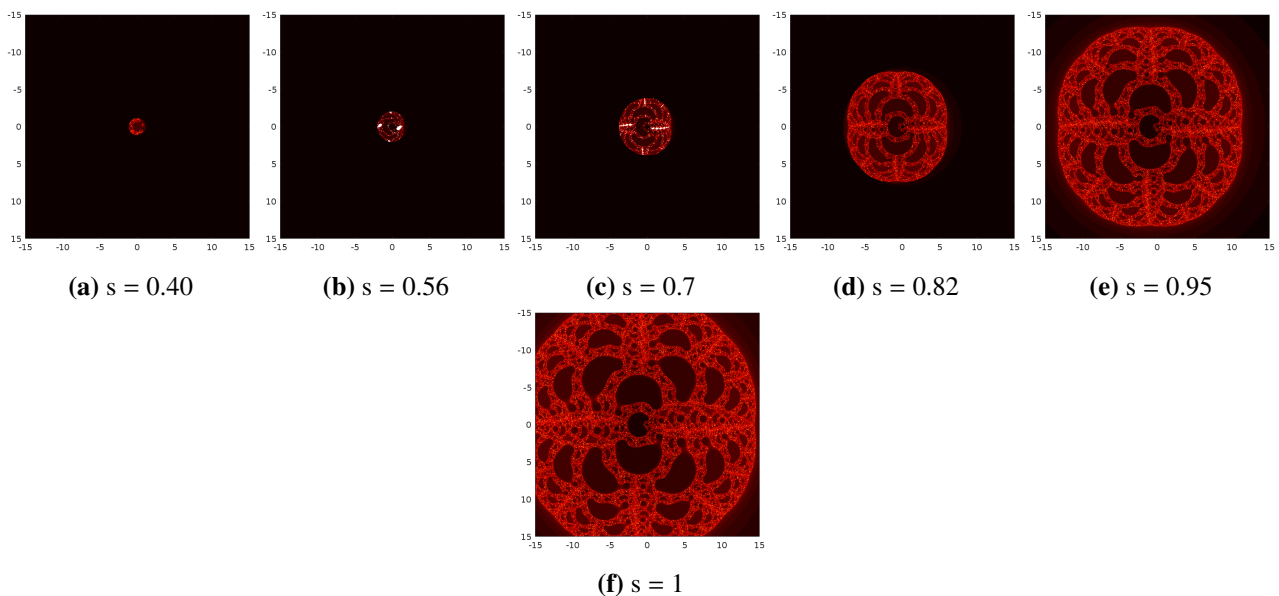


Figure 15. Generated Julia set for $n = 2, m = 4$ with a viscosity approximation iteration method, incorporating s -convexity, setting both p and q to 0.9, and adjusting s .

Next, we proceed to generate a cubic viscosity Julia set for generalized rational type mapping using Algorithm 1. The parameters used for generating this set are $n = 3, m = 5, a = 1.03, b = 0.05 - 0.09i$,

$c = 3i, \alpha = 0.0006, \beta = 0.0004$.

The illustration showcases a division into three distinct groups. In the first set, presented in Figure 16, constant values of $q = 0.5, s = 1$ are maintained, while the parameter p is varied. Specifically: (a) 0.42, (b) 0.7, (c) 0.89.

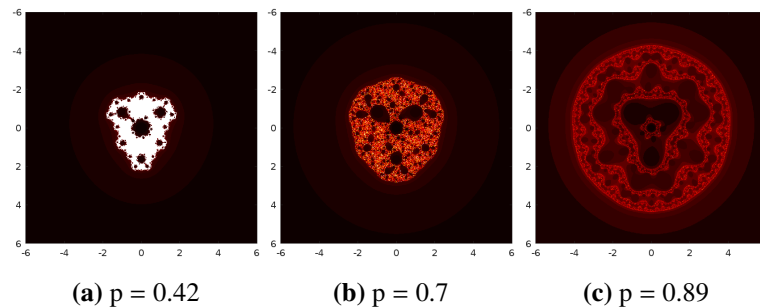


Figure 16. Julia set for $n = 3, m = 5$ created using viscosity approximation iteration with s -convexity, fixing $q = 0.5$ and $s = 1$, while adjusting p .

In the second set, presented in Figure 17, constant values of $p = 0.7, s = 1$ are maintained, while the parameter q is varied. Specifically: (a) 0.6, (b) 0.84, (c) 0.91.

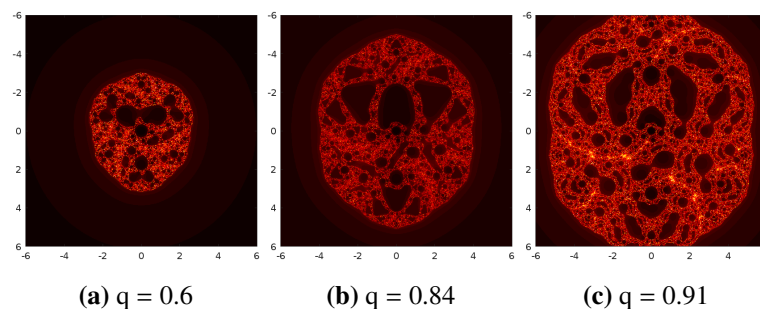


Figure 17. Julia sets for $n = 3, m = 5$ are generated using viscosity approximation orbit extended with s -convexity, with fixed parameters $p = 0.7$ and $s = 1$, while varying q .

In the third set, presented in Figure 18, constant values of $p = 0.9, q = 0.84$ are maintained, while the parameter s is varied. Specifically: (a) 0.5, (b) 0.8, (c) 1.

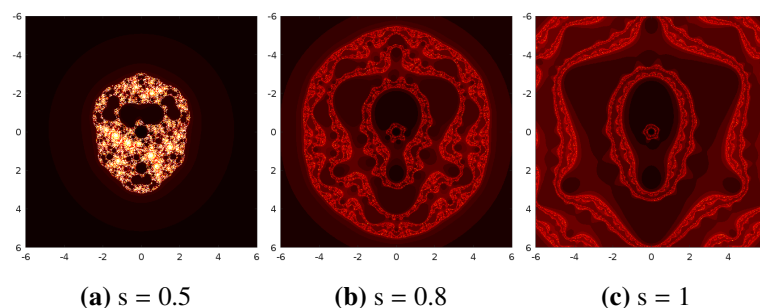


Figure 18. Julia set for $n = 3, m = 5$ generated using the viscosity approximation type iteration extended with s -convexity by fixing $p = 0.9, q = 0.84$ and varying s .

Furthermore, to show the impact of α, β on exploration of the Julia set, we apply the subsequent

parameters $n = 2$, $m = 2$, $a = 4$, $b = 0.08 + 0.09i$, $c = 0.9$, $s = 1$, $q = 0.7$, $p = 0.9$, and $\alpha = 0.8$ fixed, while we vary the value of β across six settings: (a) 0.5 , (b) $2.0089i$, (c) $4i$, (d) $5.0089i$, (e) $0.7 - 7i$, (f) $7i$. Figure 19 is obtained by fixing $\alpha = 0.8$, $s = 1$ and varying the values of β .

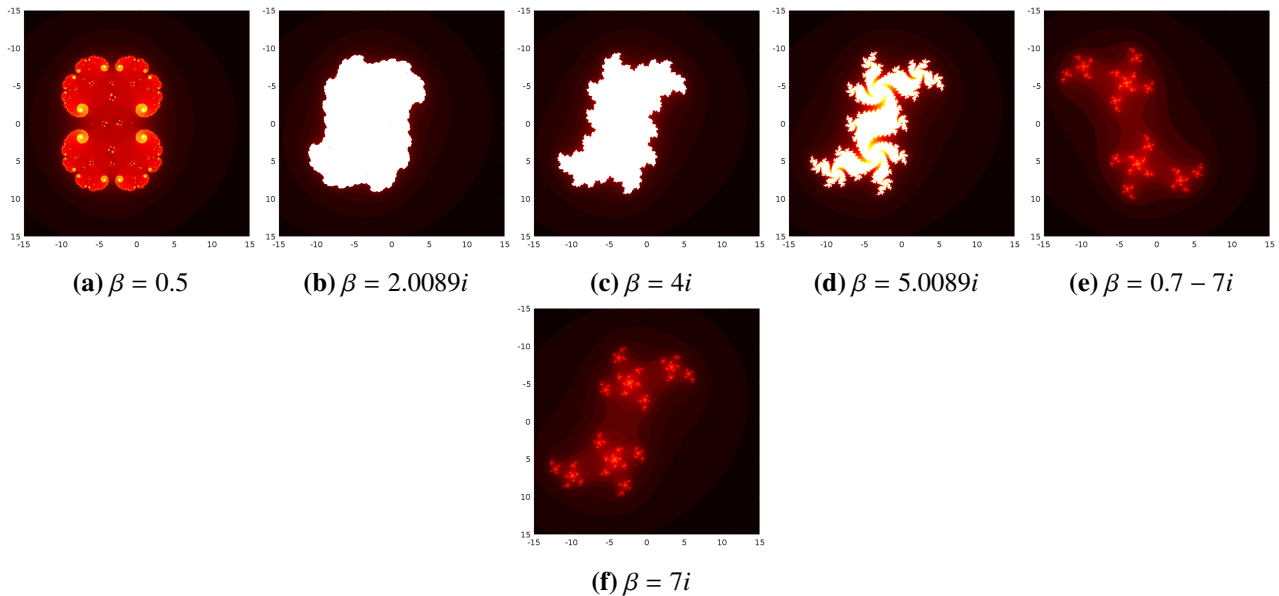


Figure 19. Julia set for $n = 2$, $m = 2$ generated using the viscosity approximation type iteration extended with s -convexity by fixing $\alpha = 0.8$, $s = 1$ and varying β .

By fixing the parameters $n = 2$, $m = 2$, $a = 4$, $b = 0.08 + 0.09i$, $c = 0.9$, $s = 1$, $q = 0.7$, $p = 0.9$, and $\beta = 5i$ and changing the value of α across three settings: (a) 0.03 , (b) 0.6 , (c) 0.9 , Figure 20 has been obtained.

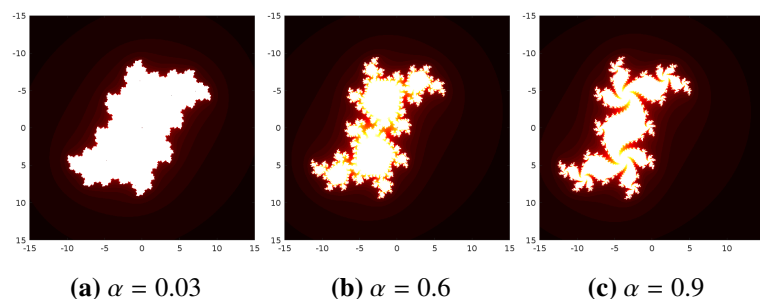


Figure 20. Julia set for $n = 2$, $m = 2$ generated using the viscosity approximation type iteration extended with s -convexity by fixing $\beta = 5i$, $s = 1$ and varying α .

Next, we move on to the exploration of the Julia set for fixed p , q , and s on different values of a , b , c . Here, we fix the following values $n = 7$, $m = 5$, $s = 0.89$, $q = 0.9$, $p = 0.8$, $\alpha = 0.8$, $\beta = 0.9i$. In Figure 21, to explore (a), (b), (c), we use $b = 0.000097 + 0.00009i$, $c = 0.990789i$ for varying $a = 2, 3, 5$. To explore (d), (e), we use $a = 2$ and $c = 0.990789i$ for different values of $b = 2.098 + 0.9989i, 0.098i$. To explore (f), we use $a = 2$ and $b = 0.000097 + 0.00009i$ for a value of $c = 2.908i$.

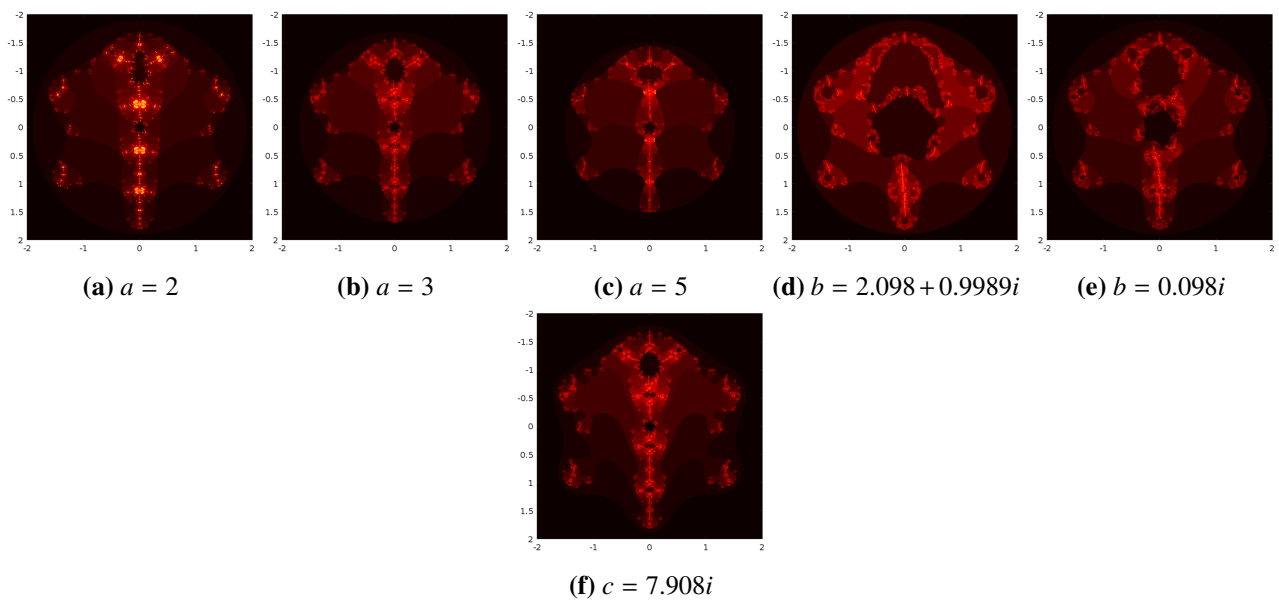


Figure 21. Julia set for $n = 7, m = 5$ explored using the viscosity approximation type iteration extended with s -convexity by fixing p, q, s and varying a, b, c .

Continuing our investigation, we venture into a countless number of viscosity Julia sets meticulously crafted using our methodology. For a comprehensive visual representation of these sets, please check Figure 22. Find below the specific parameter values employed in their generation:

- (a) $n = 3, m = 2, a = 4, b = 0.0007 + 0.006i, c = 0.0004 + 0.003i, \alpha = 0.8, \beta = 2.0089i, p = 0.7, q = 0.89,$ and $s = 0.78$.
- (b) $n = 3, m = 2, a = 9, b = 0.0007 + 0.006i, c = 0.0004 + 0.003i, \alpha = 0.8, \beta = 2.0089i, p = 0.7, q = 0.89,$ and $s = 0.78$.
- (c) $n = 4, m = 5, a = 2, b = 0.7, c = 0.1, \alpha = 0.9, \beta = 0.1, p = 0.9, q = 0.7,$ and $s = 0.88$.
- (d) $n = 6, m = 2, a = 4, b = 0.0007 + 0.006i, c = 0.0004 + 0.003i, \alpha = 0.6, \beta = 0.004, p = 0.8, q = 0.6,$ and $s = 0.4$.
- (e) $n = 6, m = 2, a = 5, b = 0.7, c = 0.3, \alpha = 0.6, \beta = 0.4, p = 0.5, q = 0.6,$ and $s = 0.89$.
- (f) $n = 7, m = 6, a = 8, b = 1.0009 - 0.0008i, c = 2.009 - 0.896i, \alpha = 0.7, \beta = 0.8, p = 0.8, q = 0.8,$ and $s = 1$.
- (g) $n = 6, m = 2, a = 5, b = 0.7, c = 0.3, \alpha = 0.6, \beta = 0.4, p = 0.8, q = 0.8,$ and $s = 0.89$.
- (h) $n = 11, m = 2, a = 5, b = 0.7, c = 0.3, \alpha = 0.6, \beta = 0.4, p = 0.8, q = 0.8,$ and $s = 0.89$.
- (i) $n = 9, m = 3, a = 7, b = -0.0009, c = 0.0002, \alpha = 0.7, \beta = 0.4, p = 0.7, q = 0.8,$ and $s = 1$.

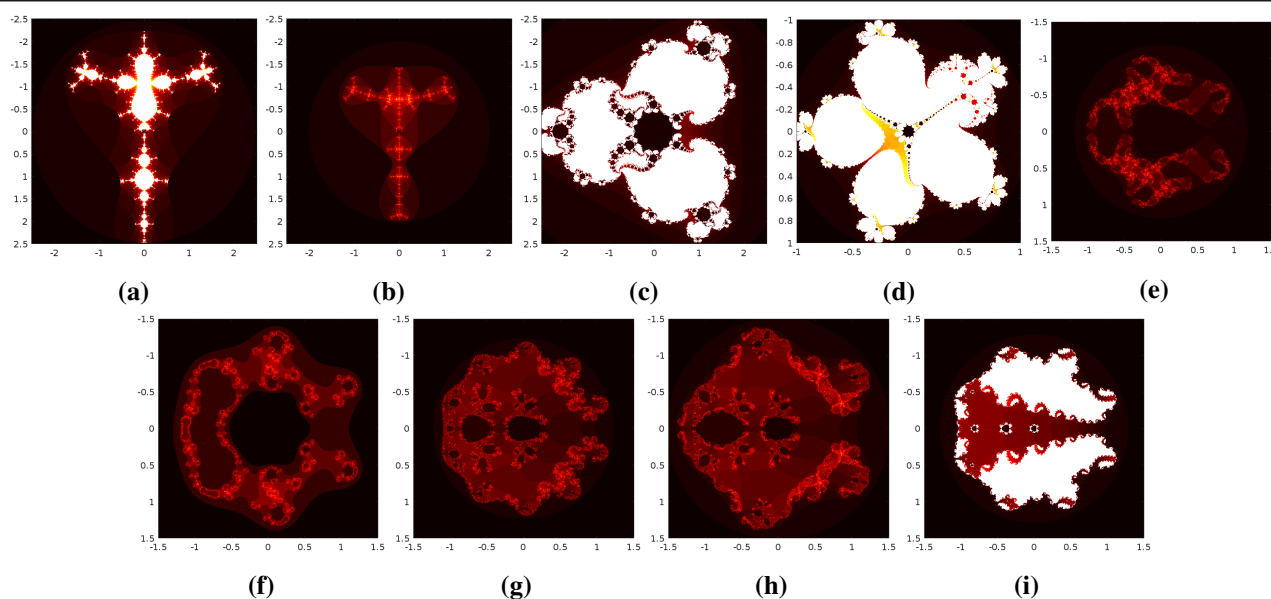


Figure 22. More examples of Julia set for viscosity approximation type iteration extended with s -convexity.

3.4.1. Results and discussion on Julia set

In Figure 13, it's apparent that a decrease in the value of p notably enhances the aesthetic appeal of the fractals, adding to their visual allure. Figures 14 and 15 underscore a pronounced relationship between the iteration parameters and the configuration of the resulting set. Particularly noteworthy is the trend where smaller parameter values correspond to compact sets, which progressively grow larger with parameter increments. Also, we can see that there's a wide range of variation in shape. In the same line, we can see the impact of parameters p, q , and s from Figures 16–18. Also, we explore the Julia set in Figures 19–21 by varying parameters of contraction and parameters of the rational type complex polynomial condition. There we can see the diversity in shape is readily apparent, producing collections that exhibit a broad spectrum of forms and intricate nuances.

From Figures 13 to 22, it is clear that each parameter, especially p, q, s and a, b, c, α, β , plays a pivotal role in shaping the Julia set and determining its overall size. Notably, as the value of the variable parameter increases, the set undergoes a notable transformation, losing its coherence and gradually resembling scattered fragments akin to dust. Furthermore, there exists a rich array of shapes exhibited by the constant function across various parameter configurations.

3.5. Mathematical description about the effect of change of parameters in the sets generated

Notable increase in the value of p , while we fix the other parameters influences the color mapping function used in visualizing the fractal. It varies the complexity of the Julia sets. Smaller values of p produce clearer and brighter regions in the fractals. Additionally, the resulting sets exhibit notable axial symmetry (Figure 3).

Increase in the value of q by fixing a, b, α, β, p , and s for $n = 3, m = 2$ leads to more defined and stable fractal patterns (Figure 4).

Increase in s and fixation of $a, b, \alpha, \beta, p, q, m$, and n leads to more defined and structured fractal

shapes (Figure 5).

The generated sets in Figure 10 are symmetrical about the X -axis. It can be observed that with small values of p with $n = 3, m = 2$, there is a clarity and brightness in the structure. However, as we increase p , the size increases but brightness is the same. For small p , the set will be more connected and colorful, while for larger p , the set will expand in complexity and brightness (Figure 13).

Change in q affects the shape and structure of the fractals, but connectivity is not lost for increased values of q (Figure 14).

When varying s , there is a growth in the set and it is symmetrical about both the axes (Figure 15).

A rotation of the fractal, for complex values of β with negative imaginary part and a dust-like structure while changing the complex values of β , can be observed, i.e., the set loses its connectivity (Figure 19).

4. Conclusions

In this study, we have explored the visualization of Mandelbrot and Julia sets using a generalized rational-type complex polynomial. We have employed an extended viscosity approximation method, enhanced by s -convexity, a technique that has been widely recognized for determining fixed points in nonlinear operators. We have introduced an escape criterion specifically designed for the generation of Mandelbrot and Julia sets through this method. Additionally, we have utilized the escape time algorithm in conjunction with our iterative process to visualize these fractal sets. The study has further investigated how changes in the parameters have affected the morphology of the produced sets and presented our observations through graphical analysis. In forthcoming research, we intend to introduce numerical measures enabling the examination of how alterations in set shape correlate with variations in the iteration parameters for our iterative orbit. Through these measures, we aim to demonstrate that the relationship within our designated iteration method exhibits pronounced non-linearity. Furthermore, we plan to expand upon the findings presented in the paper by exploring additional types of viscosity approximation orbits and their applications.

Author contributions

Arunachalam Murali: Original draft; Krishnan Muthunagai: Review & editing. All authors have read and approved the final version of the manuscript for publication.

Use of AI tools declaration

The authors declare they have not used Artificial Intelligence (AI) tools in the creation of this article.

Acknowledgments

This work was completed without any financial support from funding sources. We are also thankful to anonymous reviewers and editors for their constructive comments and suggestions that help us to improve the manuscript.

Conflict of interest

The authors declare that there is no conflict of interests regarding the publication of this paper.

References

1. A. Husain, M. N. Nanda, M. S. Chowdary, M. Sajid, Fractals: An eclectic survey, part-I, *Fractal Fract.*, **6** (2022), 89. <https://doi.org/10.3390/fractalfract6020089>
2. A. Husain, M. N. Nanda, M. S. Chowdary, M. Sajid, Fractals: An eclectic survey, part II, *Fractal Fract.*, **6** (2022), 379. <https://doi.org/10.3390/fractalfract6070379>
3. P. Fatou, Sur les substitutions rationnelles, *Comp. Rend. Heb. S. Acad. Sci.*, **164** (1917), 806–808.
4. G. Julia, Memoire sur l'iteration des fonctions rationnelles, *J. Math. Pures Appl.*, **1** (1918), 47–245.
5. B. Mandelbrot, *The fractal geometry of nature*, San Francisco: W. H. Freeman, 1982.
6. W. Mann, Mean value methods in iteration, *Proc. Am. Math. Soc.*, **4** (1953), 506–510. <https://doi.org/10.1090/S0002-9939-1953-0054846-3>
7. B. Halpern, Fixed points of nonexpanding maps, *Bull. Am. Math. Soc.*, **73** (1967), 957–961. <https://doi.org/10.1090/S0002-9904-1967-11864-0>
8. A. Moudafi, Viscosity approximation methods for fixed-points problems, *J. Math. Anal. Appl.*, **241** (2000), 46–55. <https://doi.org/10.1006/jmaa.1999.6615>
9. M. Romera, G. Pastor, G. Alvarez, F. Montoya, Growth in complex exponential dynamics, *Comput. Graph.*, **24** (2000), 115–131. [https://doi.org/10.1016/S0097-8493\(99\)00142-9](https://doi.org/10.1016/S0097-8493(99)00142-9)
10. M. Abbas, H. Iqbal, M. De la Sen, Generation of Julia and Mandelbrot sets via fixed points, *Symmetry*, **12** (2020), 86. <https://doi.org/10.3390/sym12010086>
11. L. K. Mork, D. J. Ulness, Visualization of Mandelbrot and Julia sets of Möbius transformations, *Fractal Fract.*, **5** (2021), 73. <https://doi.org/10.3390/fractalfract5030073>
12. D. J. Prajapati, S. Rawat, A. Tomar, M. Sajid, R. C. Dimri, A brief study on Julia sets in the dynamics of entire transcendental function using Mann iterative scheme, *Fractal Fract.*, **6** (2022), 397. <https://doi.org/10.3390/fractalfract6070397>
13. H. Qi, M. Tanveer, W. Nazeer, Y. Chu, Fixed point results for fractal generation of complex polynomials involving sine function via non-standard iterations, *IEEE Access*, **8** (2020), 154301–154317. <https://doi.org/10.1109/ACCESS.2020.3018090>
14. N. Hamada, F. Kharbat, Mandelbrot and Julia sets of complex polynomials involving sine and cosine functions via Picard–Mann Orbit, *Complex Anal. Oper. Theory*, **17** (2023), 13. <https://doi.org/10.1007/s11785-022-01312-w>
15. A. Tomar, V. Kumar, U. S. Rana, M. Sajid, Fractals as Julia and Mandelbrot sets of complex cosine functions via fixed point iterations, *Symmetry*, **15** (2023), 478. <https://doi.org/10.3390/sym15020478>
16. S. Rawat, D. J. Prajapati, A. Tomar, K. Gdawiec, Generation of Mandelbrot and Julia sets for generalized rational maps using SP-iteration process equipped with s -convexity, *Math. Comput. Simulation*, **220** (2024), 148–169. <https://doi.org/10.1016/j.matcom.2023.12.040>

17. M. Tanveer, W. Nazeer, K. Gdawiec, On the Mandelbrot set of $z^p + \log c^t$ via the Mann and Picard–Mann iterations, *Math. Comput. Simulation*, **209** (2023), 184–204. <https://doi.org/10.1016/j.matcom.2023.02.012>
18. A. Tassaddiq, General escape criteria for the generation of fractals in extended Jungck–Noor orbit, *Math. Comput. Simulation*, **196** (2022), 1–14. <https://doi.org/10.1016/j.matcom.2022.01.003>
19. S. Kumari, K. Gdawiec, A. Nandal, M. Postolache, R. Chugh, A novel approach to generate Mandelbrot sets, Julia sets and biomorphs via viscosity approximation method, *Chaos Solitons Fractals*, **163** (2022), 112540. <https://doi.org/10.1016/j.chaos.2022.112540>
20. S. Kumari, M. Kumari, R. Chugh, Dynamics of superior fractals via Jungck SP orbit with s -convexity, *An. Univ. Craiova Ser. Mat. Inform.*, **46** (2019), 344–365.
21. A. Nandal, R. Chugh, M. Postolache, Iteration process for fixed point problems and zeros of maximal monotone operators, *Symmetry*, **11** (2019), 655. <https://doi.org/10.3390/sym11050655>
22. S. Kumari, K. Gdawiec, A. Nandal, N. Kumar, R. Chugh, On the viscosity approximation type iterative method and its non-linear behaviour in the generation of Mandelbrot and Julia sets, *Numer. Algor.*, **96** (2024), 211–236. <https://doi.org/10.1007/s11075-023-01644-4>
23. M. R. Pinheiro, s -Convexity–foundations for analysis, *Differ. Geom. Dyn. Syst.*, **10** (2008), 257–262.
24. P. Mainje, The viscosity approximation process for quasi-nonexpansive mappings in Hilbert spaces, *Comput. Math. Appl.*, **59** (2010), 74–79. <https://doi.org/10.1016/j.camwa.2009.09.003>
25. R. L. Devaney, *A first course in chaotic dynamical systems: Theory and experiment*, 1 Eds., Boca Raton: CRC Press, 2018. <https://doi.org/10.1201/9780429503481>
26. H. O. Peitgen, H. Jürgens, D. Saupe, *Chaos and fractals: New frontiers of science*, New York: Springer, 2004. <https://doi.org/10.1007/b97624>



AIMS Press

©2024 the Author(s), licensee AIMS Press. This is an open access article distributed under the terms of the Creative Commons Attribution License (<https://creativecommons.org/licenses/by/4.0>)